An Artificial Neural Network Prediction Model of GFRP Residual Tensile Strength

Muataz I. Ali
Deparment of Civil Engineering, College of Engineering, University of Baghdad, Iraq | Deparment of Civil Engineering, College of Engineering, University of Samarra, Iraq
muitaz88@gmail.com (corresponding author)

Abbas A. Allawi
Deparment of Civil Engineering, College of Engineering, University of Baghdad, Iraq
a.allawi@uobaghdad.edu.iq

Received: 26 September 2024 | Revised: 8 October 2024 | Accepted: 13 October 2024

ABSTRACT

This study uses an Artificial Neural Network (ANN) to examine the constitutive relationships of the Glass Fiber Reinforced Polymer (GFRP) residual tensile strength at elevated temperatures. The objective is to develop an effective model and establish fire performance criteria for concrete structures in fire scenarios. Multilayer networks that employ reactive error distribution approaches can determine the residual tensile strength of GFRP using six input parameters, in contrast to previous mathematical models that utilized one or two inputs while disregarding the others. Multilayered networks employing reactive error distribution technology assign weights to each variable influencing the residual tensile strength of GFRP. Temperature exerted the most significant influence at 100%, while sample dimensions had a minimal impact at 17.9%. In addition, the mathematical model closest to the proposed was the Bazli model, because the latter depends on two variables (thickness and temperature). The ANN accurately predicted the residual tensile strength of GFRP at elevated temperatures, achieving a correlation coefficient of 97.3% and a determination coefficient of 94.3%.

Keywords-artificial neural networks;fire; GFRP, elevated temperatures; prediction model; transition temperature

I. INTRODUCTION

Fiber Reinforced Polymer (FRP) composites are advantageous materials offering numerous benefits compared to conventional ones. FRP composites have fiber reinforcement, including glass, carbon, or aramid, contained within a polymeric resin, usually consisting of polyester, epoxy, or vinyl ester [1-4]. The initial component provides elasticity and strength, whereas the subsequent component preserves fiber alignment, especially during compression, and ensures uniform stress distribution within the material [5-7]. pultruded Glass FRP (GFRP) profiles exhibit considerable potential for civil engineering applications due to their lightweight composition, strength, superior insulating properties, resilience in adverse conditions, and low maintenance requirements [8-10]. Pultruded GFRP profiles are controversial in civil engineering because of their fire performance. Few studies have evaluated the mechanical and fire behavior of GFRP material at high temperatures and connections [11-13]. One-way slab studies in [14-19] were performed below the glass transition and decomposition temperatures of GFRP. Although some fire simulations have been carried out, more is needed to accurately predict the thermal and mechanical responses of the GFRP members. In [18, 20, 21] the compressive behavior of the pultruded profile was simulated using a finite element model. In [15, 19], the mechanical response of GFRP multicellular slabs was modeled, whereas in [22] the fire behavior of the pultruded GFRP beam was simulated analytically [23-25].

Artificial Neural Networks (ANNs) are recognized as a fundamental instrument for regression problems due to their strong learnability after substantial training. ANNs have recently been employed in civil engineering for many purposes, including the prediction of concrete qualities [26-28], identifying structural damage [29], forecasting the compressive strength of concrete subjected to prolonged sulfate exposure [30], assessing chloride diffusivity in high-performance concrete [12], measuring the permeability of asphalt concrete, modeling material behavior, and optimizing structural designs [26]. ANNs have exhibited encouraging results in modeling intricate domains and have yielded highly accurate predictions using untrained data. Employing regression methods to forecast nonlinear material properties is an essential research avenue for construction materials. Recently, self-compacting mortar has gained prominence in construction [27]. Numerous studies employed mathematical models to predict the tensile strength of GFRP with a limited number of components [15, 18-22].

This study aims to predict the residual tensile strength of GFRP using an ANN with six input parameters, in contrast to the mathematical models proposed in previous studies, which relied on one or two inputs and neglected the rest. The accuracy of the previous models was less than that of the proposed model because they did not take into account all the inputs affecting the result of the residual tensile strength.

II. MODEL DEVELOPMENT USING ANN

An ANN was employed to assess and predict the effect of variables on the residual tensile strength in the GFRP section. The ANN determined the variables to be inputted and predicted the residual tensile strength of the GFRP. Neural networks possess self-regulation capabilities [27]. This approach utilized a feed-forward neural network design composed of interconnected neuron layers. Every neuron in a layer is interconnected with all neurons in the subsequent layer, although there are no connections among neurons within the same layer. The conventional architecture of these networks comprises three neural layers: the input layer, the hidden layer, and the output layer. Data are transmitted from the input layer to the hidden layer. Figure 1 illustrates the flow of information from the hidden layer to the output layer. SPSS was used to build the ANN.

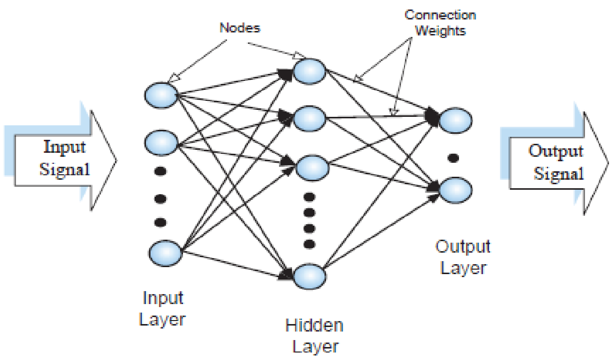

Fig. 1. Architecture of the ANN.

TABLE I. DEFINITION OF VARIABLES IN THE ANN

Variables	Type	Symbol	Sub-variables: Variables	Sub-variables: Symbol
% Residual strength	Output	*%P*		
Temperature test	Input	*T*		
Glass transition temperature	Input	*Tg*		
GFRP type	Input	*Gt*	Pultruded	1
			Bar	2
			Laminate	3
Fibres orientation	Input	*Fo*	Unidirectional	1
			Woven	2
			Chopped strand mat	3
Resin type	Input	*Rt*	Polyester	1
			Vinyl ester	2
			Epoxy	3
			Other	0
Specimen dimensions (mm)	Input	*D*		
Time test (min)	Input	*Ti*		
% Resin to fiber	Input	*Rf*		

III. STATISTICAL STUDY USING ANNS

The input model comprises the independent variables specified in Table I. The output data represent the residual strength ratio for GFRP. The data were split into three sets: a training group, charged with adjusting the weights of the ANN, a testing group, which ensures the network's performance; and a validation group to assess the model's performance. Training stopped when the error increased within the testing group.

IV. DATA COLLECTION AND DISTRIBUTION

Data were collected based on the experimental tests in [9, 18, 20, 22, 31-47]. A trial-and-error method was employed to determine the data distribution ratio for each of the three groups to enhance the performance of the ANN. The objective was to achieve the maximum correlation coefficient (*r*), which quantifies the accuracy of the projected residual strength ratio for GFRP from the network output to the actual residual strength ratio.

V. BUILDING THE MODEL

Table I shows the independent variables in the input model. The output was the residual strength. The training group adjusts ANN weights, the testing group ensures network performance by stopping training when the error increases, and the validation group evaluates model performance [30]. Table II shows the data distribution ratios for the three groups, which are needed to maximize the ANN performance and achieve the maximum correlation coefficient (*r*). This demonstrates the degree of accuracy in the relationship between the anticipated residual strength (network output) and the actual residual strength. Table II shows that the training group exhibits the highest performance at 84%, followed by the testing group at 12%, and the validation group at 4%. This assessment is based on the lowest testing error ratio of 2.1% and the highest correlation coefficient of 97.3%. The 128 samples were efficiently divided into three groups using the integrated blocked, striped, and random techniques. The striped approach was chosen because of its low error rate and better correlation.

TABLE II. EFFECT OF DATA DIVISION ON THE ANN PERFORMANCE

Data Division: Training %	Data Division: Testing %	Data Division: Validation %	Training error %	Testing error %	Correlation coefficient (*r*)%
76	21	3	6.8	6.2	96.5
60	20	20	8.3	9.9	95.9
76	12	12	6.4	14.6	96.1
80	12	8	8.6	10.7	95.7
88	8	4	6.5	9.6	95.9
80	16	4	6.4	3.8	97.0
84	**12**	**4**	**5.7**	**2.1**	**97.3**
68	20	12	8.0	5.7	96.1

The important elements were retrieved using SPSS data analysis to simplify the equation from eight inputs to six. The two lowest importance ratios were excluded and the remaining were used as inputs for the proposed model. Table III illustrates the relevance of each input. The GFRP type *Gt* and the resin to fiber *Rf* were removed since they had the lowest ratios (3.9% and 10.6%).

TABLE III. INDEPENDENT VARIABLE IMPORTANCE IN THE ANN MODEL

Input	Symbol	Importance	Normalized importance
Glass transition temperature	*Tg*	0.108	26.7%
Temperature test	*T*	0.405	100.0%
GFRP Type	*Gt*	0.016	3.9%
Fibres Orientation	*Fo*	0.160	39.5%
Resin Type	*Rt*	0.109	26.9%
Specimen Dimensions (mm)	*D*	0.082	20.1%
Time Test (min)	*Ti*	0.077	19.0%
% Resin to fiber	*Rf*	0.043	10.6%

The input layer has six neurons and the output has one, the residual strength. Several methods were employed to discover the ideal count of ANN nodes. The best identification technique is to use (1) [29], which selects a single hidden layer node and incrementally increases neural nodes until the network achieves maximum performance. The following equation yielded 13 neural nodes as the maximum number.

$$Max.No.of\ Node = 1 + 2 \times I \quad (1)$$

where I denotes the amount of parameters on the input layer.

The intermediate layer, or hidden layer, has a tan hyperbolic transfer function with a 0.4 learning rate and 0.9 momentum term. Table IV shows the correlation coefficient and testing error ratios for this layer.

TABLE IV. IMPACT OF THE NUMBER OF NEURONS IN THE HIDDEN LAYER ON ANN EFFICIENCY

No. of nodes	% Training error	% Testing error	Correlation coefficient (*r*)%
1	5.8	11.1	95.6
2	5.1	11.8	97.0
3	**5.7**	**2.1**	**97.3**
4	9.1	4.2	96.2
5	7.3	20.4	96.4
6	6.5	3.6	96.2
7	6.7	3.8	95.2
8	7.7	4.8	94.6
9	5.2	10.8	96.8
10	5.7	14.1	94.6
11	9.6	14.3	95.1
12	7.4	22.9	92.3
13	6.0	13.3	96.2

Table IV indicates that the ANN performed optimally with three neural nodes in the hidden layer, exhibiting the maximum correlation coefficient (r) at 97.3% and the lowest error ratio at 2.1%. The estimated residual strength of GFRP comprised six neurons in the input layer, three in the hidden layer, and one in the output layer, as shown in Figure 2.

VI. RESIDUAL TENSILE STRENGTH MODEL

The connection between each neuron and another has a weight that indicates the importance of the connection. Each neuron combines all the products after multiplying each input value from the neurons in the layer above by the relevant connection weights. Upon completion of the ANN training, neural node weights were acquired, encompassing interactions between the input and hidden layers, as well as the weights linking the hidden and output layers, as seen in Table V.

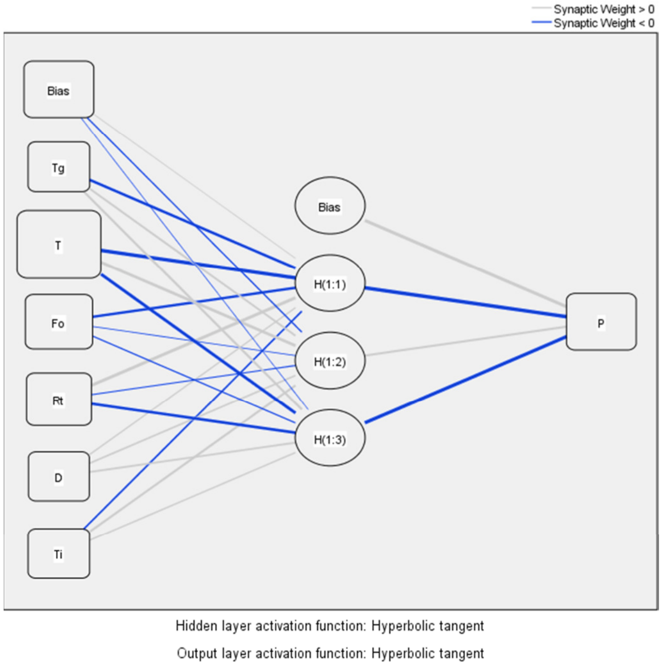

Fig. 2. Neural network for residual strength of GFRP.

TABLE V. WEIGHTS OF THE LINK BETWEEN LAYERS AND THRESHOLD LIMITS

Predictor		Predicted			
		Hidden Layer			Output Layer
		H(1:1)	H(1:2)	H(1:3)	% P
Input Layer	(Bias)	0.056	-0.137	-0.039	
	Tg	-0.542	0.380	0.533	
	T	-1.087	0.603	-0.652	
	Gt	-0.540	-0.049	-0.135	
	Fo	0.748	-0.112	-0.587	
	Rt	0.144	0.278	0.325	
	D	-0.245	0.472	0.175	
Hidden Layer	(Bias)				**0.779**
	H(1:1)				**-1.147**
	H(1:2)				**0.469**
	H(1:3)				**-0.789**

It is important to note that during the training phase, all inputs (*Tg*, *T*, *Fo*, *Rt*, *D*, and *Ti*) were changed from their actual values to relative values within the range of (-1, 1) in compliance with the criteria of SPSS. This adjustment was completed using the weights (W_i) and the threshold limit (*Bias*) listed in Table V. Thus, the equations (2)-(4)were produced. To acquire the actual values of *%P* outputs, the relative value of the output was modified using (5).

$$H_1 = Tanh[(-0.054.Tg) - (0.004.T) - (0.540.Fo) + (0.748.Rt) + (0.052.D) + (0.005.Ti) + 4.877] \quad (2)$$

$$H_2 = Tanh[(0.038.Tg) + (0.002.T) - (0.049.Fo) - (0.112.Rt) - (0.052.D) + (0.005.Ti) - 4.071] \quad (3)$$

$$H_3 = Tanh[(0.053.Tg) - (0.002.T) - (0.135.Fo) - (0.587.Rt) + (0.061.D) + (0.002.Ti) - 2.092] \quad (4)$$

$$\%P_{GFRP} = \{[Tanh[-(1.147.H1) + (0.469.H2) - (0.789.H3) + 0.779] * 46\} + 48 \quad (5)$$

The retrieved values were validated using statistical criteria, including MAPE, AA%, R^2, and R to confirm the accuracy of the equation generated by the ANN. Equations (6) and (7) were employed to compute the MAPE and AA percentages.

$$MAPE = \frac{\left(\sum\left|\frac{A-E}{A}\right|\right)*100}{n} \quad (6)$$

$$AA\% = 100\,\% - MAPE \quad (7)$$

where A denotes the actual values of $\%P$, E denotes the values of $\%P$ calculated by (5), and n denotes the number of samples. The average accuracy percentage (AA%) is determined using (7).

Table VI shows the validation model statistical standards for 8% of the samples. The results show that the ANN equation for GFRP $\%P$ residual strength is 92.3% accurate. The proposed model matches the practical results, as shown in Figure 3.

TABLE VI. ANN VALIDATION RESULTS

Statistical standards	Correlation coefficient (R)	Determination coefficient (R^2)	Mean Absolute Percentage Error (MAPE)	Average Accuracy percentage (AA %)
Statistical value for ANN	97.3	94.3	7.7	92.3

After verifying the model, SPSS was used to get the essential ratios to determine how each input affects the equation's output. Table VII shows that temperature T had the most significant impact of 100%. However, the sample dimensions D had the most minor influence at 17.9 %.

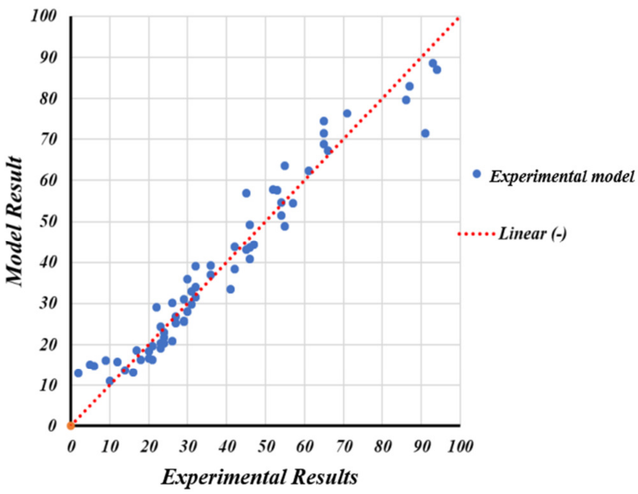

Fig. 3. Agreement between the practical results and the proposed model.

TABLE VII. INDEPENDENT VARIABLE IMPORTANCE IN THE ANN MODEL

Input	Symbol	Importance	Normalized importance
Glass transition temperature	Tg	0.089	20.6%
Temperature test	T	0.431	100.0%
Fibres Orientation	Fo	0.176	40.9%
Resin Type	Rt	0.140	32.5%
Specimen Dimensions (mm)	D	0.077	17.9%
Time Test (min)	Ti	0.087	20.3%

Figure 4 shows the mathematical models adopted in [20, 34, 48-50] compared to the proposed model. It should be noted that the closest mathematical model to the proposed is the Bazli model because it depends on two variables (thickness and temperature) unlike the rest of the models that relied on only temperature or temperature and glass transition temperature Tg, which had an importance of 20.6 % as previously mentioned.

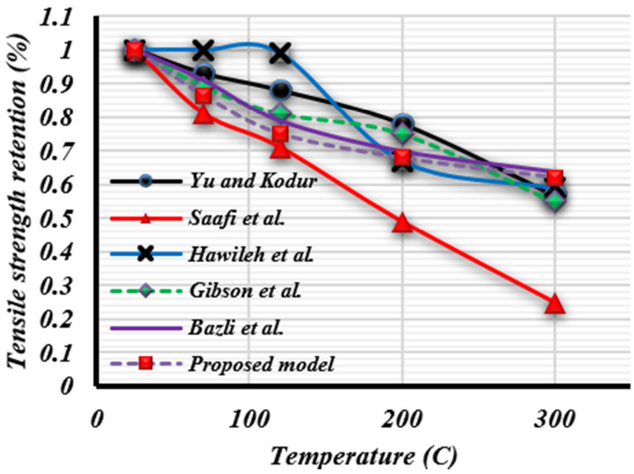

Fig. 4. Proposed model vs previous models.

VII. CONCLUSIONS

After collecting the data and training the ANN model, weights were obtained for each input to build a mathematical model, concluding the following:

- The variables Gt and Rf had the least significance with importance ratios of 3.9% and 10.6%. So they were excluded, reducing the model inputs from eight to six.
- The optimal number of neurons in the hidden layer of the ANN is 13.
- The ANN model demonstrated 92.3% accuracy in predicting the GFRP $\%P$ residual strength, confirming the efficiency of the proposed model.
- The proposed model was close to Bazli's model, which considered both thickness and temperature, making it more accurate than models relying solely on temperature.

- The proposed model aligns well with practical results demonstrating its reliability in real-world applications.

REFERENCES

[1] A. Hussein Ali Al-Ahmed, A. Al-Rumaithi, A. A. Allawi, and A. El-Zohairy, "Mesoscale analysis of Fiber-Reinforced concrete beams," *Engineering Structures*, vol. 266, Sep. 2022, Art. no. 114575, https://doi.org/10.1016/j.engstruct.2022.114575.

[2] T. H. Ibrahim, A. A. Allawi, and A. El-Zohairy, "Experimental and FE analysis of composite RC beams with encased pultruded GFRP I-beam under static loads," *Advances in Structural Engineering*, vol. 26, no. 3, pp. 516–532, Feb. 2023, https://doi.org/10.1177/13694332221130795.

[3] E. M. Mahmood, A. A. Allawi, and A. El-Zohairy, "Analysis and Residual Behavior of Encased Pultruded GFRP I-Beam under Fire Loading," *Sustainability*, vol. 14, no. 20, Jan. 2022, Art. no. 13337, https://doi.org/10.3390/su142013337.

[4] S. D. Mohammed, T. H. Ibrahim, B. F. Salman, A. A. Allawi, and A. El-Zohairy, "Structural Behavior of Reactive Powder Concrete under Harmonic Loading," *Buildings*, vol. 13, no. 8, Aug. 2023, Art. no. 1917, https://doi.org/10.3390/buildings13081917.

[5] M. I. Ali, A. A. Allawi, and A. El-Zohairy, "Flexural Behavior of Pultruded GFRP–Concrete Composite Beams Strengthened with GFRP Stiffeners," *Fibers*, vol. 12, no. 1, Jan. 2024, Art. no. 7, https://doi.org/10.3390/fib12010007.

[6] M. Bazli *et al.*, "Durability of glass-fibre-reinforced polymer composites under seawater and sea-sand concrete coupled with harsh outdoor environments," *Advances in Structural Engineering*, vol. 24, no. 6, pp. 1090–1109, Apr. 2021, https://doi.org/10.1177/1369433220947897.

[7] Z. H. Dakhel and S. D. Mohammed, "Castellated Beams with Fiber-Reinforced Lightweight Concrete Deck Slab as a Modified Choice for Composite Steel-Concrete Beams Affected by Harmonic Load," *Engineering, Technology & Applied Science Research*, vol. 12, no. 4, pp. 8809–8816, Aug. 2022, https://doi.org/10.48084/etasr.4987.

[8] S. I. Ali and A. A. Allawi, "Effect of Web Stiffeners on The Flexural Behavior of Composite GFRP- Concrete Beam Under Impact Load," *Journal of Engineering*, vol. 27, no. 3, pp. 76–92, Feb. 2021, https://doi.org/10.31026/j.eng.2021.03.06.

[9] H. Ashrafi, M. Bazli, A. Jafari, and T. Ozbakkaloglu, "Tensile properties of GFRP laminates after exposure to elevated temperatures: Effect of fiber configuration, sample thickness, and time of exposure," *Composite Structures*, vol. 238, Apr. 2020, Art. no. 111971, https://doi.org/10.1016/j.compstruct.2020.111971.

[10] T. H. Ibrahim, I. A. S. Alshaarbaf, A. A. Allawi, N. K. Oukaili, A. El-Zohairy, and A. I. Said, "Theoretical Analysis of Composite RC Beams with Pultruded GFRP Beams subjected to Impact Loading," *Engineering, Technology & Applied Science Research*, vol. 13, no. 6, pp. 12097–12107, Dec. 2023, https://doi.org/10.48084/etasr.6424.

[11] H. H. Ali and A. M. I. Said, "Flexural behavior of concrete beams with horizontal and vertical openings reinforced by glass-fiber-reinforced polymer (GFRP) bars," *Journal of the Mechanical Behavior of Materials*, vol. 31, no. 1, pp. 407–415, Jan. 2022, https://doi.org/10.1515/jmbm-2022-0045.

[12] M. I. Ali, A. A. J. Jamel, and S. I. Ali, "The hardened characteristics of self-compacting mortar including carbon fibers and estimation results by artificial neural networks," *AIP Conference Proceedings*, vol. 2213, no. 1, Mar. 2020, Art. no. 020159, https://doi.org/10.1063/5.0000177.

[13] A. A. Allawi and S. I. Ali, "Flexural Behavior of Composite GFRP Pultruded I-Section Beams under Static and Impact Loading," *Civil Engineering Journal*, vol. 6, no. 11, pp. 2143–2158, Nov. 2020, https://doi.org/10.28991/cej-2020-03091608.

[14] J. J. Massot, "Glass reinforced plastics heavy load flooring for offshore platforms," presented at the Matériaux composites dans l'industrie pétrolière 1994.

[15] T. Keller, C. Tracy, and E. Hugi, "Fire endurance of loaded and liquid-cooled GFRP slabs for construction," *Composites Part A: Applied Science and Manufacturing*, vol. 37, no. 7, pp. 1055–1067, Jul. 2006, https://doi.org/10.1016/j.compositesa.2005.03.030.

[16] T. Morgado, J. R. Correia, N. Silvestre, and F. A. Branco, "Experimental study on the fire resistance of GFRP pultruded tubular beams," *Composites Part B: Engineering*, vol. 139, pp. 106–116, Apr. 2018, https://doi.org/10.1016/j.compositesb.2017.11.036.

[17] J. R. Correia, Y. Bai, and T. Keller, "A review of the fire behaviour of pultruded GFRP structural profiles for civil engineering applications," *Composite Structures*, vol. 127, pp. 267–287, Sep. 2015, https://doi.org/10.1016/j.compstruct.2015.03.006.

[18] P. M. H. Wong and Y. C. Wang, "An experimental study of pultruded glass fibre reinforced plastics channel columns at elevated temperatures," *Composite Structures*, vol. 81, no. 1, pp. 84–95, Nov. 2007, https://doi.org/10.1016/j.compstruct.2006.08.001.

[19] Y. Bai and T. Keller, "Delamination and kink-band failure of pultruded GFRP laminates under elevated temperatures and compression," *Composite Structures*, vol. 93, no. 2, pp. 843–849, Jan. 2011, https://doi.org/10.1016/j.compstruct.2010.07.010.

[20] A. G. Gibson, M. E. O. Torres, T. N. A. Browne, S. Feih, and A. P. Mouritz, "High temperature and fire behaviour of continuous glass fibre/polypropylene laminates," *Composites Part A: Applied Science and Manufacturing*, vol. 41, no. 9, pp. 1219–1231, Sep. 2010, https://doi.org/10.1016/j.compositesa.2010.05.004.

[21] J. V. Bausano, J. J. Lesko, and S. W. Case, "Composite life under sustained compression and one sided simulated fire exposure: Characterization and prediction," *Composites Part A: Applied Science and Manufacturing*, vol. 37, no. 7, pp. 1092–1100, Jul. 2006, https://doi.org/10.1016/j.compositesa.2005.06.013.

[22] Y. Bai, T. Vallée, and T. Keller, "Modeling of thermal responses for FRP composites under elevated and high temperatures," *Composites Science and Technology*, vol. 68, no. 1, pp. 47–56, Jan. 2008, https://doi.org/10.1016/j.compscitech.2007.05.039.

[23] T. H. Ibrahim, A. A. Allawi, and A. El-Zohairy, "Impact Behavior of Composite Reinforced Concrete Beams with Pultruded I-GFRP Beam," *Materials*, vol. 15, no. 2, Jan. 2022, Art. no. 441, https://doi.org/10.3390/ma15020441.

[24] E. M. Mahmood, A. A. Allawi, and A. El-Zohairy, "Flexural Performance of Encased Pultruded GFRP I-Beam with High Strength Concrete under Static Loading," *Materials*, vol. 15, no. 13, Jan. 2022, Art. no. 4519, https://doi.org/10.3390/ma15134519.

[25] E. M. Mahmood, T. H. Ibrahim, A. A. Allawi, and A. El-Zohairy, "Experimental and Numerical Behavior of Encased Pultruded GFRP Beams under Elevated and Ambient Temperatures," *Fire*, vol. 6, no. 5, May 2023, Art. no. 212, https://doi.org/10.3390/fire6050212.

[26] B. Rezaul, K. Joarder, and S. Ruhul, Neural Networks in Healthcare: Potential and Challenges: Potential and Challenges. Idea Group Inc (IGI), 2006.

[27] D. Graupe, *Principles Of Artificial Neural Networks*, 3rd ed. World Scientific, 2013.

[28] A. A. J. Jamel and M. I. Ali, "Stability and Seepage of Earth Dams with Toe Filter (Calibrated with Artificial Neural Network)," *Journal of Engineering Science and Technology*, vol. 16, no. 5, pp. 3712–3725, 2021.

[29] A. S. Saadoon and H. S. Malik, "Prediction of Ultimate Load of Concrete Beams Reinforced with FRP Bars Using Artificial Neural Networks," *Al-Qadisiyah Journal for Engineering Sciences*, vol. 10, no. 1, 2017.

[30] A. M. Ahmed, S. I. Ali, M. I. Ali, and A. A. J. Jamel, "Analyzing Self-Compacted Mortar Improved by Carbon Fiber Using Artificial Neural Networks," *Annales de Chimie - Science des Matériaux*, vol. 47, no. 6, pp. 363–369, Dec. 2023, https://doi.org/10.18280/acsm.470602.

[31] S. Alsayed, Y. Al-Salloum, T. Almusallam, S. El-Gamal, and M. Aqel, "Performance of glass fiber reinforced polymer bars under elevated temperatures," *Composites Part B: Engineering*, vol. 43, no. 5, pp. 2265–2271, Jul. 2012, https://doi.org/10.1016/j.compositesb.2012.01.034.

[32] H. Ashrafi, M. Bazli, A. Vatani Oskouei, and L. Bazli, "Effect of Sequential Exposure to UV Radiation and Water Vapor Condensation and Extreme Temperatures on the Mechanical Properties of GFRP Bars," *Journal of Composites for Construction*, vol. 22, no. 1, Feb. 2018,

Art. no. 04017047, https://doi.org/10.1061/(ASCE)CC.1943-5614.0000828.

[33] F. Aydin, "Effects of various temperatures on the mechanical strength of GFRP box profiles," *Construction and Building Materials*, vol. 127, pp. 843–849, Nov. 2016, https://doi.org/10.1016/j.conbuildmat.2016.09.130.

[34] M. Bazli, H. Ashrafi, A. Jafari, X.-L. Zhao, H. Gholipour, and A. V. Oskouei, "Effect of thickness and reinforcement configuration on flexural and impact behaviour of GFRP laminates after exposure to elevated temperatures," *Composites Part B: Engineering*, vol. 157, pp. 76–99, Jan. 2019, https://doi.org/10.1016/j.compositesb.2018.08.054.

[35] E. U. Chowdhury, R. Eedson, L. A. Bisby, M. F. Green, and N. Benichou, "Mechanical Characterization of Fibre Reinforced Polymers Materials at High Temperature," *Fire Technology*, vol. 47, no. 4, pp. 1063–1080, Oct. 2011, https://doi.org/10.1007/s10694-009-0116-6.

[36] J. R. Correia, M. M. Gomes, J. M. Pires, and F. A. Branco, "Mechanical behaviour of pultruded glass fibre reinforced polymer composites at elevated temperature: Experiments and model assessment," *Composite Structures*, vol. 98, pp. 303–313, Apr. 2013, https://doi.org/10.1016/j.compstruct.2012.10.051.

[37] D. S. Ellis, H. Tabatabai, and A. Nabizadeh, "Residual Tensile Strength and Bond Properties of GFRP Bars after Exposure to Elevated Temperatures," *Materials*, vol. 11, no. 3, Mar. 2018, Art. no. 346, https://doi.org/10.3390/ma11030346.

[38] S. K. Foster and L. A. Bisby, "Fire Survivability of Externally Bonded FRP Strengthening Systems," *Journal of Composites for Construction*, vol. 12, no. 5, pp. 553–561, Oct. 2008, https://doi.org/10.1061/(ASCE)1090-0268(2008)12:5(553).

[39] H. Hajiloo, M. F. Green, and J. Gales, "Mechanical properties of GFRP reinforcing bars at high temperatures," *Construction and Building Materials*, vol. 162, pp. 142–154, Feb. 2018, https://doi.org/10.1016/j.conbuildmat.2017.12.025.

[40] R. J. A. Hamad, M. A. Megat Johari, and R. H. Haddad, "Mechanical properties and bond characteristics of different fiber reinforced polymer rebars at elevated temperatures," *Construction and Building Materials*, vol. 142, pp. 521–535, Jul. 2017, https://doi.org/10.1016/j.conbuildmat.2017.03.113.

[41] R. A. Hawileh, A. Abu-Obeidah, J. A. Abdalla, and A. Al-Tamimi, "Temperature effect on the mechanical properties of carbon, glass and carbon–glass FRP laminates," *Construction and Building Materials*, vol. 75, pp. 342–348, Jan. 2015, https://doi.org/10.1016/j.conbuildmat.2014.11.020.

[42] M. Jarrah, E. P. Najafabadi, M. H. Khaneghahi, and A. V. Oskouei, "The effect of elevated temperatures on the tensile performance of GFRP and CFRP sheets," *Construction and Building Materials*, vol. 190, pp. 38–52, Nov. 2018, https://doi.org/10.1016/j.conbuildmat.2018.09.086.

[43] Z. Lu, G. Xian, and H. Li, "Effects of elevated temperatures on the mechanical properties of basalt fibers and BFRP plates," *Construction and Building Materials*, vol. 127, pp. 1029–1036, Nov. 2016, https://doi.org/10.1016/j.conbuildmat.2015.10.207.

[44] I. Nause, "Determination of Temperature-Dependent Tensile Strengths of ComBAR Reinforcement Bars; Report No: 072/05-Nau-3740/6345," Brunswick Institute for Concrete Material Testing, Germany, 072/05-Nau-3740/6345, 2005.

[45] F. M. Özkal, M. Polat, M. Yağan, and M. O. Öztürk, "Mechanical properties and bond strength degradation of GFRP and steel rebars at elevated temperatures," *Construction and Building Materials*, vol. 184, pp. 45–57, Sep. 2018, https://doi.org/10.1016/j.conbuildmat.2018.06.203.

[46] M. Robert and B. Benmokrane, "Behavior of GFRP Reinforcing Bars Subjected to Extreme Temperatures," *Journal of Composites for Construction*, vol. 14, no. 4, pp. 353–360, Aug. 2010, https://doi.org/10.1061/(ASCE)CC.1943-5614.0000092.

[47] M. Shekarchi, E. M. Farahani, M. Yekrangnia, and T. Ozbakkaloglu, "Mechanical strength of CFRP and GFRP composites filled with APP fire retardant powder exposed to elevated temperature," *Fire Safety Journal*, vol. 115, Jul. 2020, Art. no. 103178, https://doi.org/10.1016/j.firesaf.2020.103178.

[48] R. A. Hawileh, J. A. Abdalla, S. S. Hasan, M. B. Ziyada, and A. Abu-Obeidah, "Models for predicting elastic modulus and tensile strength of carbon, basalt and hybrid carbon-basalt FRP laminates at elevated temperatures," *Construction and Building Materials*, vol. 114, pp. 364–373, Jul. 2016, https://doi.org/10.1016/j.conbuildmat.2016.03.175.

[49] M. Saafi, "Effect of fire on FRP reinforced concrete members," *Composite Structures*, vol. 58, no. 1, pp. 11–20, Oct. 2002, https://doi.org/10.1016/S0263-8223(02)00045-4.

[50] B. Yu and V. Kodur, "Effect of temperature on strength and stiffness properties of near-surface mounted FRP reinforcement," *Composites Part B: Engineering*, vol. 58, pp. 510–517, Mar. 2014, https://doi.org/10.1016/j.compositesb.2013.10.055.